DANISH METEOROLOGICAL INSTITUTE

SCIENTIFIC REPORT

00- 05

Advection Experiments with DMI-HIRLAM-TRACER

Jérôme Chenevez

COPENHAGEN 2000

ISSN-Nr. 0905-3263 (printed)
ISSN Nr. 1399-1949 (online)
ISBN-Nr. 87-7478-409-9

SUMMARY

This study investigates the possibility of using DMI-HIRLAM for the transport of passive tracers in the perspective of developing an Eulerian atmospheric long-range dispersion model for prevision of air-pollution episodes. In the present work the model resulting from the implementation of passive scalars in DMI-HIRLAM is tested with different advection schemes applied to a field of one passive tracer. Simulations of the first European Tracer Experiment (ETEX), which supplies the most suitable data for such an investigation, are performed to compare model results with actual observations.

In a first step the Eulerian central difference scheme operating by default in DMI-HIRLAM-TRACER is tested and it is improved by adding vertical diffusion processes. Although good qualitative results are obtained with this formulation, it presents very bad mass conservation properties. In a second step an improved numerical scheme of the advection, the Bott scheme, is implemented inside the semi-Lagrangian model version of DMI-HIRLAM-TRACER. Because of its good mass conservation and its low computation cost, this formulation turns out to be the most suitable of the ones tested to simulate the transport of pollutants in the atmosphere.

LIST OF CONTENTS

1. Introduction

Eulerian atmospheric long-range dispersion models have been used by several meteorological institutes to predict air pollution episodes. At DMI, air-pollution forecast models like DERMA and DACFOS [1,2], which are based on a 3-D Lagrangian transport model [3], use HIRLAM meteorological forecasts in an off-line fashion. Though such Lagrangian models may have lower computer costs, Eulerian models are the most suitable to deal with pollution processes known on a grid (like for example emission data). Eulerian modelling presents the characteristic to be complete in the sense that all the physical processes involved can be included at each point of the model volume. A subsequent advantage of Eulerian models is that they can display pollutant distribution over the entire modelled region and not only along trajectories. The purpose for the present project is to investigate the possibility of using the DMI-HIRLAM model in a mesoscale air-pollution forecast system. This is done by the development of DMI-HIRLAM-TRACER (shortened as TRACER in the following), which is a version of DMI-HIRLAM implemented with advection/diffusion of passive tracers. A further aim, not considered here, is to integrate HIRLAM as a meteorological driver in a coupled (also called "on-line") meteorological/chemical Eulerian atmospheric transport and chemistry model system.

The main objective of this work is to exercise the advection scheme of HIRLAM by simulating the transport of passive tracers in the model. A convenient way, commonly used in literature to test an advection scheme, is to simulate the transport of a simple structure in, for example, a non-divergent circular wind field. Such artificial conditions are not appropriate with an advanced model like HIRLAM, for they would not allow to investigate the complete properties of the model. A more suitable and realistic way to test the transport of a field of passive tracers is supplied by the European Tracer Experiments (ETEX -1&2) performed in 1994. As a first step the default advection-diffusion schemes operating in TRACER will be tested on ETEX-1 data and the results will be compared with those of other model simulations, as well as with measurements during the experiment. In a second step an attempt will be made to ameliorate the performances of the default advection scheme used in TRACER by applying an improved numerical scheme developed by Bott [4,5]. This scheme has been implemented and experimented following a method used at MISU [6,7]. Because of its mass conservation and low diffusion properties, this scheme is one of the most suitable for transport of pollutants in the atmosphere.

Additional processes could also be taken into account by adding sources and sinks terms in the right hand side of the advection-diffusion equation in order to describe chemical processes, as well as emission and deposition processes. In other words one could integrate a chemistry module in TRACER. Such extensions are left for further developments of the model.

The present work has been done using the "recoded" version of DMI-HIRLAM [8] in which an additional module has been included to handle the emission and the transport of a field of one passive tracer. The conditions of the simulations of the ETEX experiment are briefly summarised in the next section. The implementation of the emission of the passive tracers is outlined in section 3. Simulations performed in the default Eulerian set-up of TRACER and improvements obtained by applying different vertical and horizontal diffusion profiles to the passive tracers are presented in section 4. Section 5 is devoted to simulations performed in the semi-Lagrangian time integration mode and improved with the Bott's advection scheme. The results obtained from the different simulations are discussed in section 6. Finally, some conclusions are drawn in the last section.

2. The ETEX release

The first ETEX release started on October 23rd 1994 16:00 GMT in Brittany (France) and had a duration of 11 hours and 50 minutes. The precise location of the release was (2.0083°W, 48.0583°N) and it was on the ground at 90 m above sea level. The total amount of material released was 340 kg of Perfluoro-Methyl-Cyclo-Hexane (PMCH) corresponding to a release rate of 7.95 g/sec. The release was followed during 3 days by a series of measurements of the concentration at specific locations in Europe from which it was possible to observe the cloud evolution [9].

The numerical experiments performed in the present work begin 4 hours before the start of the ETEX release by using initial meteorological fields from the European Centre for Medium-Range Weather Forecasts (ECMWF) of October 23rd 1994 12:00 GMT. They were carried out during 66 hours by updating the lateral boundaries from ECMWF every 6 hours (using 6-hour forecasts and new analysis every 12 hours). The numerical simulations were performed with TRACER over a model region covering Europe, in a grid with 50×48 points yielding an horizontal resolution of 0.4° (about 42km × 44km) ; all experiments were performed using a 31-level resolution in a hybrid vertical coordinate system.

Indications about the performances of these simulations are here given by 1) the geographical position on the surface (more precisely at the lowest model level, about 30 m above the ground in the present version of DMI-HIRLAM) of the modelled concentration field at different forecast times after the start of the release, 2) the value and 3-dimensional position at each time step of the maximum concentration point, 3) the total area mean value of the vertically integrated concentration per unit horizontal area (called *average concentration* in the following), which is given at each time step by the diagnostic calculations of the model and 4) a time-series of 1-hour averaged concentrations "observed" at a specific model point corresponding to the site of Risø in Denmark. The first and last of these results can be compared to real measurements and/or results of other models [9,10], while the other two may allow an evaluation of the stability and the confidence of different schemes.

3. Emission of the passive tracers

3.1 Geometrical outlook

Since the conditions of the release are exactly known (location, total mass and rate of the release), the main difficulty is to perform such a local release inside an Eulerian grid point model. It is necessary to assume uniform distribution of the tracer within the volume of the grid box inside which the release is initiated. The knowledge of this volume makes it possible to calculate the concentration of the passive tracer, in order to compare the simulated tracer field with the observed concentration field.

The specific data for the emission of the tracer (location, duration and release rate) are inputs of the model and the release is by default performed at the lowest model level ; the altitude of the emission point is then 32 m over the ground. This approximation on the actual altitude of the release is assumed to have no effect on the results if we can assume that the release occurs inside a well-mixed Atmospheric Boundary Layer.

From the geographical coordinates of the release location, it is easy to find the 4 closest grid points that define the horizontal grid cell (at the lowest level of the vertical grid in the case of a release on the ground) in which the release point is located. The altitudes of these 4 points at each of the two lowest levels are then calculated via the geopotential. The knowledge of the altitude of the 2nd lowest level is necessary to calculate the volume of the grid box. Depending

on if the actual release location is closer to the middle of a grid cell or closer to a grid point, one can choose to use as source of the emission, either the 4 closest grid points, or only the first closest point respectively. It turns out that this choice has a small effect, mainly in the beginning of the transport when the tracers are still close to the source. In this study it was chosen, so as to compare the different experiments independently of this source parameter, to keep only one single emission point in every case.
Knowing the release rate (mass per time unit) one can thus calculate the concentration change per time step inside the grid box around the emission point. It is obvious that, since the volume of the emitting grid box depends on the grid resolution, the initial concentration (or emitted concentration) also depends on the grid resolution. But since the concentration is as well calculated from the release rate, it then depends on the length of a time step, that itself also depends on the grid resolution. To put it in a nutshell, the higher the resolution is, the higher the emitted concentration will be. This influence of the grid resolution on the concentration is mainly visible close to the source when the whole concentration field is contained only in one or a few grid boxes. It tends to disappear away from the source when the field disseminates in the model and the average concentration decreases.

3.2 Computational outlook

The equation to be solved is the advection-diffusion equation driving the dynamic evolution of the concentration of a passive tracers field:

$$\frac{\partial \mathrm{C}}{\partial \mathrm{t}} = -\nabla(\mathbf{v}\mathrm{C}) + \nabla(\mathbf{K}\nabla\mathrm{C}) + Q + S \tag{1}$$

vector **v** represents the advecting velocity field, **K** is the 3 dimensional eddy diffusivity, Q and S represent source and sink terms respectively. Note that there is at present no sink included, so S=0. In the next subsection we will focus on the advective part of this equation, but for our present purpose we only need to describe the emission part, that is:

$$\frac{\partial \mathrm{C}_{\mathrm{i,j,k}}}{\partial \mathrm{t}} = Q_{\mathrm{i,j,k}} \tag{2}$$

where $\mathrm{C_{i,j,k}}$ is the concentration at a point (i,j,k) of the 3-D grid and the source term $\mathrm{Q_{i,j,k}}$ represents here the emission of the passive tracers. In the present case $\mathrm{Q_{i,j,k}}$ is equal to the release rate (Q) at the emission point and is set to zero everywhere else.
Deriving concentration change at the emission point with the leapfrog time stepping used in the Eulerian scheme of HIRLAM gives:

$$\frac{C^p - C^m}{2\tau} = Q \tag{3}$$

where τ is the dynamic time step of the scheme. This is a 3-time level scheme where the value of the concentration at time level t-1 is represented by $\mathrm{C^m}$, the value at time t by $\mathrm{C^z}$ and the value at time t+1 by $\mathrm{C^p}$. The value at time t+1 of the concentration at the emission point is thus given by:

$$C^p = 2\tau Q + C^m \tag{4}$$

That is the emitted concentration at the current time step plus the remaining concentration from the previous time step. Hence, during the duration of the emission, the value of the concentration at the emission point is forced by equation (4). In the model, the evolution of the concentration is computed separately from the value of the emission parameter Q which depends on the volume of the emitting grid box.

There can be other situations where the emission is not only localised at a single point but rather distributed over an area ; this emitting area is then considered as a group of emitting points where the concentration is computed in the same way as above.

4. The Eulerian advection scheme

4.1 Formulation with a central difference scheme

Deriving the advective part of equation (1) in a finite central difference form, it becomes:

$$\frac{\partial C_{i,j,k}}{\partial t} = -\left(\frac{u_{i+1} \cdot C_{i+1} - u_{i-1} \cdot C_{i-1}}{2\delta x} + \frac{v_{j+1} \cdot C_{j+1} - v_{j-1} \cdot C_{j-1}}{2\delta y} + \frac{w_{k+1} \cdot C_{k+1} - w_{k-1} \cdot C_{k-1}}{2\delta \eta} \right) + \nabla(\mathbf{K}\nabla C) + Q \quad (5)$$

where u, v, w are the components of the velocity vector **v**. It is not possible to use this central difference scheme in its classic form without meeting problems of mass conservation due to the staggering of the Arakawa C-grid used in HIRLAM. The equation (5) may be approximated instead as follows:

$$\begin{aligned} \frac{\partial C_{i,j,k}}{\partial t} = & -\frac{1}{2}\left(u_{i+\frac{1}{2}} \frac{C_{i+1} - C_i}{\delta x} + u_{i-\frac{1}{2}} \frac{C_i - C_{i-1}}{\delta x} \right) \\ & -\frac{1}{2}\left(v_{j+\frac{1}{2}} \frac{C_{j+1} - C_j}{\delta y} + v_{j-\frac{1}{2}} \frac{C_j - C_{j-1}}{\delta y} \right) \\ & -\frac{1}{2}\left(w_{k+\frac{1}{2}} \frac{C_{k+1} - C_k}{\delta \eta} + w_{k-\frac{1}{2}} \frac{C_k - C_{k-1}}{\delta \eta} \right) \\ & + \nabla(\mathbf{K}\nabla C) + Q \end{aligned} \quad (6)$$

Using the index convention in HIRLAM (i.e. $u_{i+1/2}$ -> u_i) the concentration in the 3-time level leapfrog scheme is thus computed by:

$$\begin{aligned} C^{p}_{i,j,k} = C^{m}_{i,j,k} & -\frac{\tau}{\delta x}(u_i(C^{z}_{i+1} - C^{z}_{i}) + u_{i-1}(C^{z}_{i} - C^{z}_{i-1})) \\ & -\frac{\tau}{\delta y}(v_j(C^{z}_{j+1} - C^{z}_{j}) + v_{j-1}(C^{z}_{j} - C^{z}_{j-1})) \\ & -\frac{\tau}{\delta \eta}(w_k(C^{z}_{k+1} - C^{z}_{k}) + w_{k-1}(C^{z}_{k} - C^{z}_{k-1})) \\ & + 2\tau(\nabla(\mathbf{K}\nabla C) + Q) \end{aligned} \quad (7)$$

τ is the length of one time step.

This is the formulation in which the advection equation is coded in the HIRLAM reference version[11]. To ensure numerical stability the time step used with this scheme must satisfy the CFL criterion (Courant number $u_i\tau/\delta x \leq 1$) in each direction. In order to avoid negative values of positive definite quantities such values are set to zero. We will discuss later the consequences of such a resetting procedure.

Note that the horizontal diffusion is computed separately in HIRLAM by an implicit 4th order scheme (eq. 2.1.4.10 in [11]), but vertical diffusion of the passive tracers is not implemented in the default version of the model.

4.2 Results.

4.2.1 Default formulation

Simulations of the ETEX release have been performed using the default formulation of the advection/diffusion equation for the passive tracers (7). In figure 1 the result for the modelled surface concentration of the simulation using ECMWF lateral boundaries updates with a resolution of 0.4° is presented at 24 and 48 hours after the start of the release.

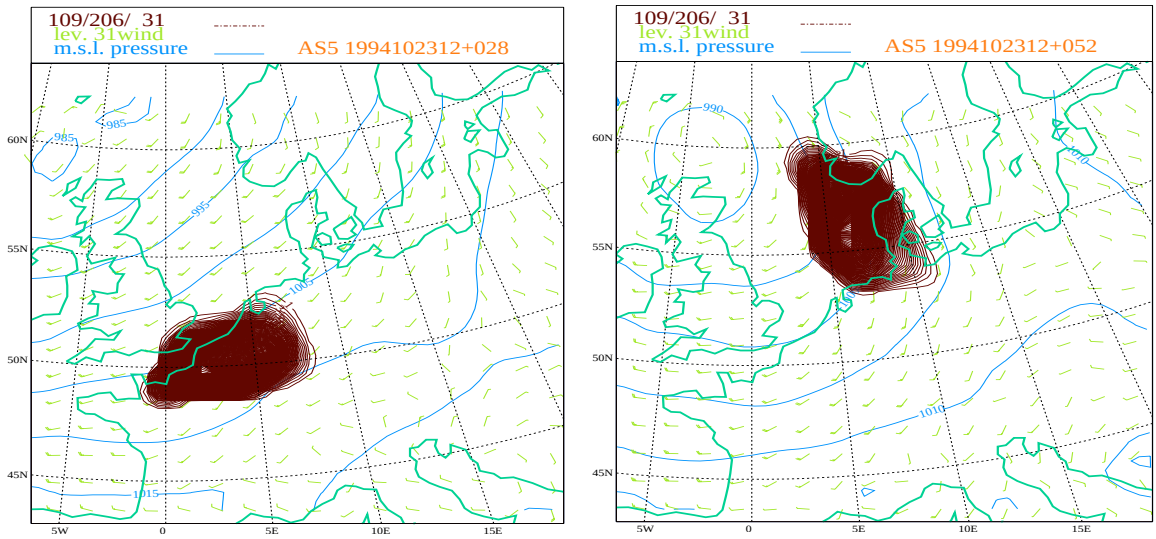

Figure 1 : Surface modelled concentration for a simulation of ETEX at 24 hours (28 hours after starting the simulation) and 48 hours after the start of the release (52 hours after start of the simulation) with the default Eulerian scheme used in TRACER and with a resolution of 0.4° ; the maximum concentrations on the surface are 187 ng/m^3 and 146 ng/m^3, respectively.

The surface concentrations obtained are about 100 times too high, and the position and the shape of the cloud of passive tracers after 48 hours do not correspond to the observations [9]. Moreover, although the value of the maximum concentration slowly decreases while the field of the passive tracer spreads out, figure 2 shows that the *average concentration* rapidly exceeds the level corresponding to the total amount of passive tracers actually emitted in the model (340 kg emitted correspond to 78.13 ng/m^2), and it still increases even after the emission is finished ; this denotes obviously a violation of the mass conservation law.

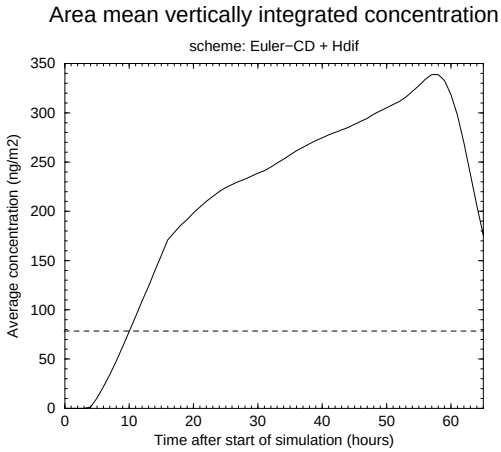

Figure 2 : Variation of the *average concentration* during the simulation reflecting the evolution of the amount of passive tracer contained in the model. The emission phase is contained between 4 hours and 16 hours after the beginning of the simulation. The decrease after 60 hours is due to the exit from the model area of a part of the passive tracers field. The horizontal dashed line indicates the *average concentration* corresponding to the total amount of passive tracers introduced in the model (78.13 ng/m^2).

4.2.2 Improvement with vertical diffusion

In the preceding simulation no vertical diffusion was applied to the passive tracers field. In the present version of TRACER, vertical diffusion for the passive tracers is implemented in the same way as it is for the cloud water. Two schemes have been tested : an improved version of the 1st order non-local Holtslag scheme [12] and a 1.5 order local turbulent kinetic energy (TKE) scheme known as the CBR scheme [13].
The previous simulation is repeated applying the vertical diffusion to the passive tracers. Figure 3 displays the modelled surface concentration 48h after the beginning of the release, obtained with the Holtslag scheme and the CBR scheme respectively.

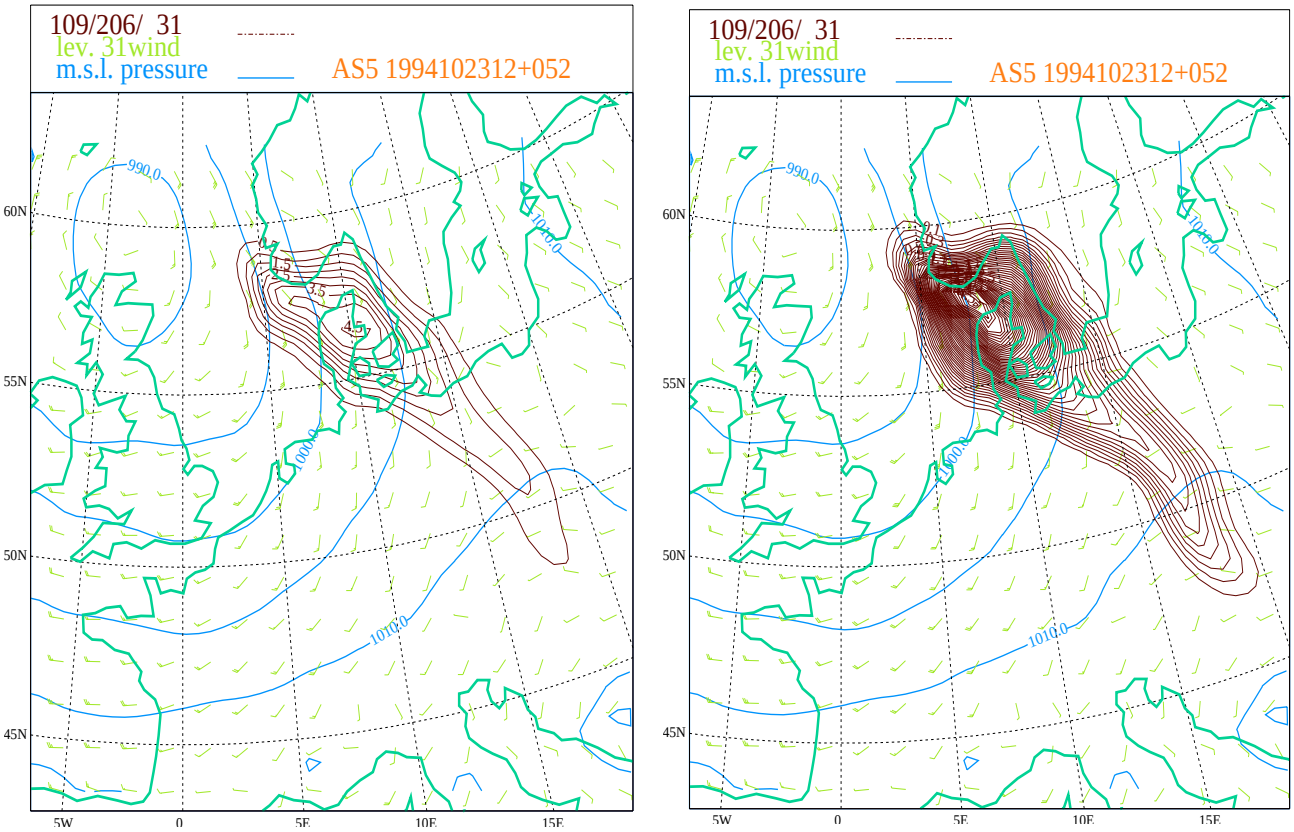

Figure 3 : Modelled surface concentration at 48 hours after the start of the release (52 hours after starting the simulation) with the Eulerian scheme and vertical diffusion. Left : Holtslag scheme. Right: CBR scheme. Because the results obtained (shapes of the clouds and maximum concentrations on the surface : 4,7 ng/m^3 and 4,9 ng/m^3, respectively) are very close to each other, and thus the plots almost identical, the numbers of isolines displayed are not the same in order to show different structures inside the clouds.

The shape and position of the cloud are rather close to the observations, but the maximum value of the surface concentration is at least two times too high according to the measurements.

Figure 4 compares the evolution of the *average concentration* obtained with the two vertical diffusion schemes. The curves are very close to each other, and compared to fig.2 the increase of the total amount of passive tracers is 30% lower than previously, but it is still 3.2 times too high, according to mass conservation.

We can conclude that the Holstlag and the CBR schemes perform similarly, and as it was expected, the use of the vertical diffusion in the transport of the passive tracers greatly improves the results.

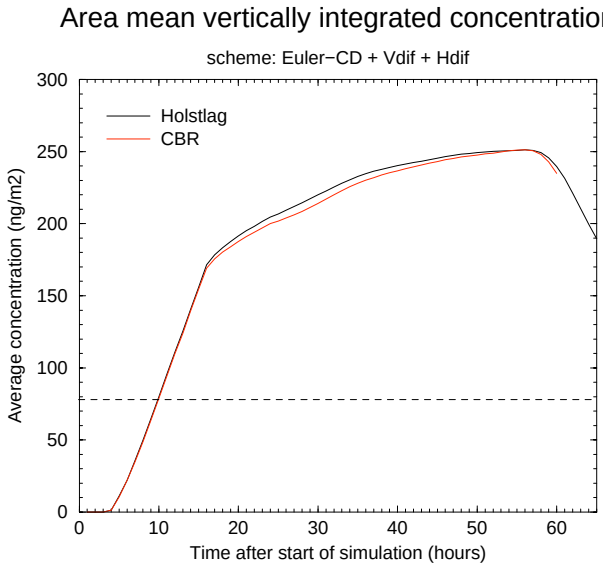

Figure 4 : Progresses of the area mean concentration during simulations using vertical diffusion for passive tracers. The horizontal dashed line shows the level corresponding to the total amount of emitted passive tracers.

4.2.3 Altering the horizontal diffusion

The horizontal diffusion coefficient ($K = 10^{14} m^2 \cdot s^{-1}$) may be modified on each model level by a factor, whose default value is equal to 1 on every level. The following simulation tests the effects of strong horizontal diffusion with a factor 4 on every level.
Figure 5 shows the modelled surface concentration field obtained 24 hours and 48 hours after the start of the release.

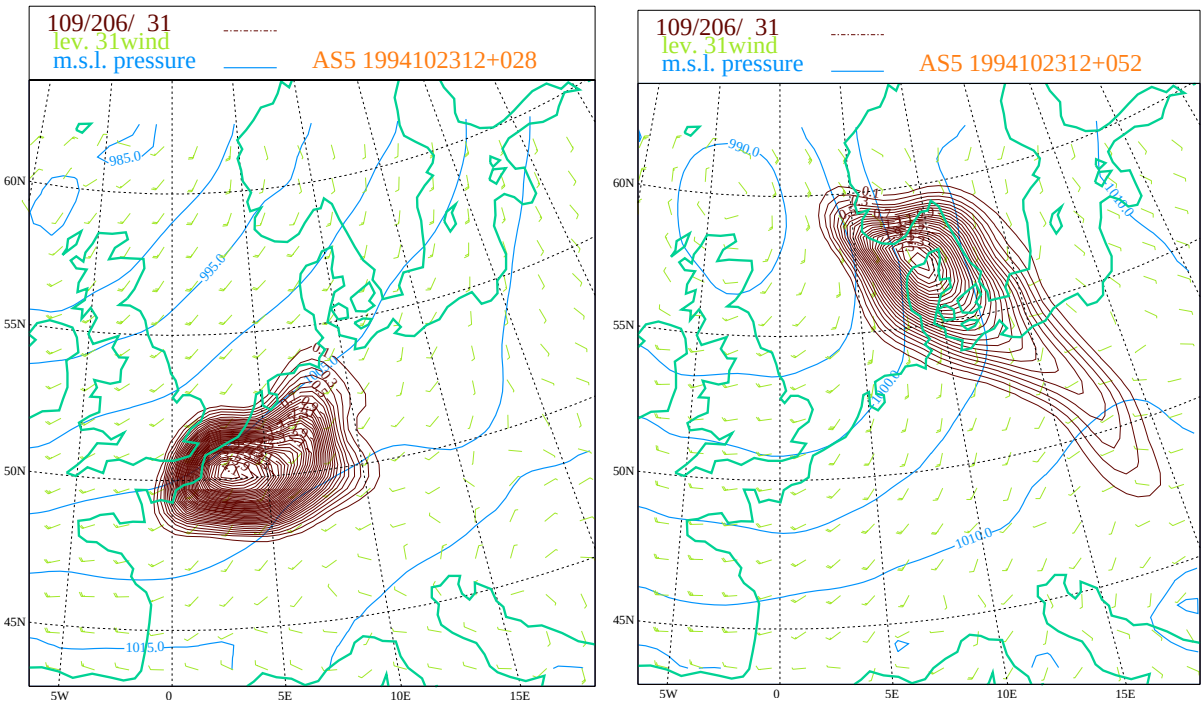

Figure 5 : Surface modelled concentration at 24 hours and 48 hours after the start of the release with horizontal diffusion factor =4, Eulerian central difference scheme for advection and CBR scheme for vertical diffusion ; the maximum concentrations on the surface are 4,3 ng/m^3 and 2,8 ng/m^3, respectively.

Compared to fig.3 (right) the passive tracers field after 48 hours is only a little wider, but the maximum surface concentration is lower as well as the horizontal gradient is smoother too; the maximum concentration is divided by almost a factor two, becoming closer to the measurements.

Figure 6 presents the variations, as a function of time after the beginning of the release, of one-hour average modelled concentrations at Risø on the lowest model level and compared to the surface observations [9] from which the background concentration has been subtracted. It displays the curves obtained with each of the two vertical diffusion schemes and with horizontal diffusion coefficient factor equal to 1 and 4, respectively. One can see that the time after which the cloud comes over Risø, around 50 hours after the beginning of the release, corresponds roughly to the observations, but the shape and the value of the peaks are very different.

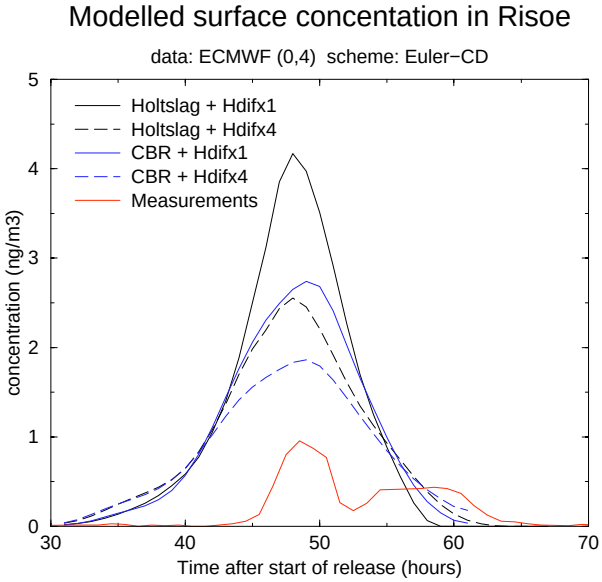

Figure 6 : Variations of one-hour average surface concentration at Risø. Modelled concentrations obtained with different horizontal diffusion coefficients and with Holtslag and CBR schemes respectively are compared to measurements from which the background concentration has been subtracted.

5. Semi-Lagrangian model

5.1 Theory

In the two-level semi-Lagrangian time scheme of HIRLAM [14,15] the equation for the concentration of the passive tracers field may be written:

$$\frac{\mathrm{dC}}{\mathrm{dt}} \equiv \frac{\partial \mathrm{C}}{\partial \mathrm{t}} + u\frac{\partial \mathrm{C}}{\partial \mathrm{x}} + v\frac{\partial \mathrm{C}}{\partial \mathrm{y}} + w\frac{\partial \mathrm{C}}{\partial \mathrm{z}} = \nabla(\mathbf{K}\nabla \mathrm{C}) + Q \tag{8}$$

In the semi-Lagrangian scheme, air-parcels are tracked back at each time step along trajectories from predicted arrival grid points to departure points. Knowing the origin of the air parcel, its corresponding concentration value is found by interpolation from the concentration value at the grid point at the previous time level. In the two-time level semi-implicit scheme, the new concentration is thus given by:

$$C^p = \tau\left[\nabla(\mathrm{K}\nabla \mathrm{C}) + \mathrm{Q}\right] + C^z \tag{9}$$

where the term in brackets is evaluated at the arrival point [11]. Here the horizontal diffusion is computed by a one way 4th order implicit filtering [14] using an equivalent horizontal diffusivity K =10^{14}m^2·s^{-1}. The CBR scheme [13] will be applied for the vertical diffusion of the passive tracers. As in the Eulerian model, unrealistic negative values of positive definite quantities are set to zero. One of the major interests of the semi-Lagrangian scheme is that the CFL criterion can be overlooked and longer time steps may thus be used.

5.2 Results

Figure 7 presents modelled surface concentration obtained at 24 and 48 hours after start of release.

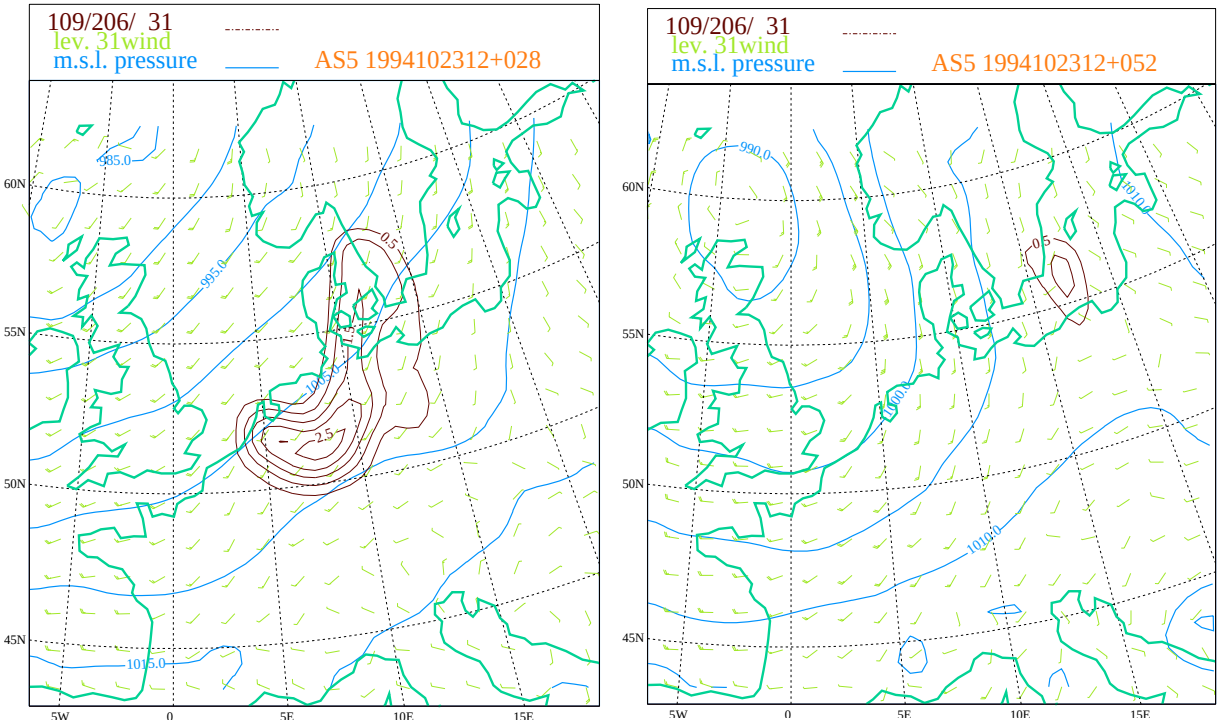

Figure 7 : Surface modelled concentration at 24 hours and 48 hours after the start of the release with the semi-Lagrangian scheme, implicit horizontal diffusion and the CBR scheme for vertical diffusion ; the maximum concentrations on the surface are 2,7 ng/m^3 and 1,2 ng/m^3, respectively.

Figure 8 shows the evolution of the *average concentration* and figure 9 reveals surface concentration variation at Risø. These results are obviously far from the observations, for the field of passive tracer rapidly fades and completely vanishes after 60 hours. The neutralisation of the vertical and/or horizontal diffusions yields similar outcomes, showing that the semi-Lagrangian scheme has to be improved in respect to the mass conservation requirement.

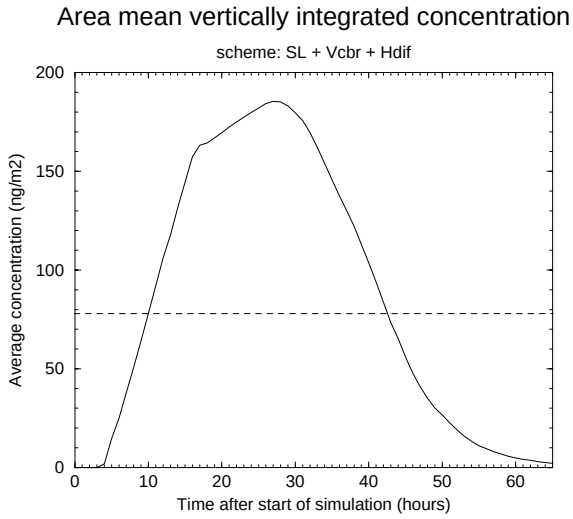

Figure 8 : *Average concentration* variation during the simulation using the semi-Lagrangian scheme with implicit horizontal diffusion and CBR vertical diffusion scheme.

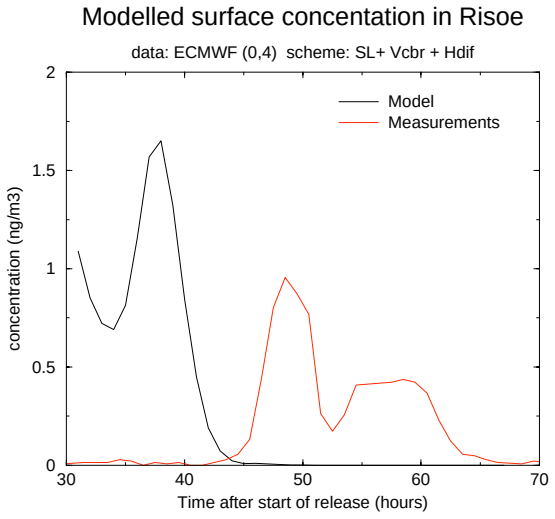

Figure 9 : Same as fig.6 showing modelled concentration obtained with the semi-Lagrangian scheme together with implicit horizontal diffusion and CBR vertical diffusion schemes.

5.3 Improvement of the advection in HIRLAM with the Bott scheme

5.3.1 Model.

With a view to improving the mass conservation of the model, a separate numerical scheme for tracer advection has been implemented in the semi-Lagrangian version of HIRLAM [6]. The Bott advection scheme [4,5] has been chosen for its flux conservation properties [16].
The Bott scheme is an Eulerian scheme for the advection, therefore, the CFL criterion has to be fulfilled in each direction and at each time step. It is inspired by the upstream method in the sense that it maintains the conservative and positive definiteness properties of the upstream scheme, but greatly reduces its numerical diffusion. Using the upstream scheme the concentration may be computed by:

$$C^{p}_{i,j,k} = C^{z}_{i,j,k} - \frac{\tau}{\delta x}(F^{z}_{i+½} - F^{z}_{i-½}) - \frac{\tau}{\delta y}(F^{z}_{j+½} - F^{z}_{j-½}) - \frac{\tau}{\delta \eta}(F^{z}_{k+½} - F^{z}_{k-½}) + \tau(\nabla(\mathbf{K}\nabla C) + Q) \quad (10)$$

where F represents a flux of concentration (C**v**), hence depending on the sign of the velocity components (u, v, w) and given by:

$$\left.\begin{aligned} F^{z}_{i+½} &= \frac{1}{2}\left[(u_{i+½} + |u_{i+½}|)C^{z}_{i} + (u_{i+½} - |u_{i+½}|)C^{z}_{i+1}\right] \\ F^{z}_{j+½} &= \frac{1}{2}\left[(v_{j+½} + |v_{j+½}|)C^{z}_{j} + (v_{j+½} - |v_{j+½}|)C^{z}_{j+1}\right] \\ F^{z}_{k+½} &= \frac{1}{2}\left[(w_{k+½} + |w_{k+½}|)C^{z}_{k} + (w_{k+½} - |w_{k+½}|)C^{z}_{k+1}\right] \end{aligned}\right\} \quad (11a)$$

$$\left.\begin{aligned} F^{z}_{i-½} &= \frac{1}{2}\left[(u_{i-½} + |u_{i-½}|)C^{z}_{i-1} + (u_{i-½} - |u_{i-½}|)C^{z}_{i}\right] \\ F^{z}_{j-½} &= \frac{1}{2}\left[(v_{j-½} + |v_{j-½}|)C^{z}_{j-1} + (v_{j-½} - |v_{j-½}|)C^{z}_{j}\right] \\ F^{z}_{k-½} &= \frac{1}{2}\left[(w_{k-½} + |w_{k-½}|)C^{z}_{k-1} + (w_{k-½} - |w_{k-½}|)C^{z}_{k}\right] \end{aligned}\right\} \quad (11b)$$

In the Bott's method (10) is still used but the advective fluxes are instead of (11) defined in the following way (for the x- direction):

$$(Cu)_{i+½} \equiv F_{i+½} = \frac{1}{\tau}\int_{x_{i+½}-u\tau}^{x_{i+½}} C_i(x)dx \quad (12)$$

This is the flux across a zone boundary at i+1/2, equal to the mass of constituent transported through the right hand boundary of the grid box i during one time step τ. The similar equation for $F_{i-1/2}$ is obtained by replacing i with i-1.
Fitting polynomials of order q are used to represent the distribution of the concentration in a grid box i:

$$C_{i,q}(x) = \sum_{p=0}^{q} a_{i,p}\left(\frac{x - x_i}{\delta x}\right)^{p} \quad (13)$$

where the coefficients $a_{q,p}$ are functions of (q+1)C-values and may be obtained by interpolating the C-curve with the aid of neighbouring grid points. They are chosen so that the area under the polynomial in grid box i equals $C_i\delta x$; their values up to the 4th degree are given in [4]. This is called the upstream form or integrated flux form of the Bott scheme.

A mass conservative representation of the passive tracer field in each grid box is obtained if area preserving polynomials are used. In this case the polynomial coefficients are determined by solving at grid point i the linear system of q+1 equations:

$$C_{l,q}\delta x = \int_{x_{l-\frac{1}{2}}}^{x_{l+\frac{1}{2}}} \sum_{p=0}^{q} a_{i,p} \left(\frac{x - x_i}{\delta x} \right)^p dx \qquad \text{with } l\text{=i, i}\pm1\text{, i}\pm2\text{, ...} \tag{14}$$

The values of the coefficients for this constant grid flux form of the Bott scheme are given up to the 4th degree in [5] in the special situation with equidistant grid spacing[1].
The concentration at time level t+1 due to advection in the x-direction may then be computed by:

$$C_i^p = \frac{\mathrm{i}_{i-\frac{1}{2}}^{+}}{\mathrm{i}_{i-1}} C_{i-1}^z + \left(1 - \frac{\mathrm{i}_{i+\frac{1}{2}}^{+} + \mathrm{i}_{i-\frac{1}{2}}^{-}}{\mathrm{i}_i} \right) C_i^z + \frac{\mathrm{i}_{i+\frac{1}{2}}^{-}}{\mathrm{i}_{i+1}} C_{i+1}^z \tag{15}$$

with

$$\begin{aligned} \mathrm{i}_{i+\frac{1}{2}}^{+} &= \max\left(0,\ \mathrm{I}_{i+\frac{1}{2}}^{+}\right) \\ \mathrm{i}_{i+\frac{1}{2}}^{-} &= \max\left(0,\ \mathrm{I}_{i+\frac{1}{2}}^{-}\right) \\ \mathrm{i}_i &= \max\left(\mathrm{I}_i, \mathrm{i}_{i+\frac{1}{2}}^{+} + \mathrm{i}_{i-\frac{1}{2}}^{-} + \varepsilon\right) \end{aligned} \tag{16}$$

where the small term $\varepsilon>0$ is introduced to avoid numerical instability when $\mathrm{i}_i=0$ and the integrals I, depending on the sign of the velocity, may be defined by writing:

$$F_{i+\frac{1}{2}} = \frac{\delta x}{\tau} \left[\frac{\mathrm{I}_{i+\frac{1}{2}}^{+}}{\mathrm{I}_i} C_i - \frac{\mathrm{I}_{i+\frac{1}{2}}^{-}}{\mathrm{I}_{i+1}} C_{i+1} \right] \tag{17}$$

which according to equations (12) and (13) yields to:

$$\mathrm{I}_{i+\frac{1}{2}}^{+} = \int_{\frac{1}{2}-c_i^{+}}^{\frac{1}{2}} C_{i,l}(x)dx = \sum_{p=0}^{l} \frac{a_{i,p}}{(p+1)2^{p+1}} \left[1 - (1-2c_i^{+})^{p+1} \right] \tag{18a}$$

$$\mathrm{I}_{i+\frac{1}{2}}^{-} = \int_{-\frac{1}{2}}^{-\frac{1}{2}+c_i^{-}} C_{i+1,l}(x)dx = \sum_{p=0}^{l} \frac{a_{i+1,p}}{(p+1)2^{p+1}} (-1)^p \left[1 - (1-2c_i^{-})^{p+1} \right] \tag{18b}$$

$$\mathrm{I}_i = \int_{-\frac{1}{2}}^{\frac{1}{2}} C_{i,l}(x)dx = \sum_{p=0}^{l} \frac{a_{i,p}}{(p+1)2^{p+1}} \left[(-1)^p + 1 \right] \tag{19}$$

where in equations (18) we have $c_i^{\pm} = \pm(c_{i+\frac{1}{2}} \pm |c_{i+\frac{1}{2}}|)/2$, in which $\mathrm{c}_{i+1/2}=\mathrm{u}_{i+1/2}\tau/\delta\mathrm{x}$ is the Courant number ; these integrals are thus constrained by the CFL criterion. The constant grid flux form of the Bott scheme is simply obtained by substituting the above coefficients $\mathrm{a}_{i,p}$ by those defined in (14) and given in [5]. Note that the terms $\mathrm{C_i/I_i}$ and $\mathrm{C_{i+1}/I_{i+1}}$ appearing in (17) are weighting factors in which $\mathrm{I_i}$ and $\mathrm{I_{i+1}}$ are equal to the integrals in (18) when $\mathrm{c}_{i\pm1/2}=\pm1$. In equation (15) the first term of the right hand side vanishes if the velocity is negative and the last term vanishes if the velocity is positive. Equations (16) ensure positive definiteness, while the mass conservation is achieved by equations (17), (18) and (19).

[1] The approximation made here by assuming equidistant grid-spacing in HIRLAM may yield a slight non-conservation of the mass, as it will be seen in the next section. This is corrected by using higher model resolution.

5.3.2 Implementation

The Bott scheme for the advection, which code for HIRLAM has generously been supplied by Annica Ekman from MISU[7], can be combined with the dynamic part of the semi-Lagrangian model, replacing the default advection scheme for the passive tracers in the semi-Lagrangian time scheme. The method described above is extended to the three dimensions by using the time splitting method in which the one dimension procedure is repeated alternatively in each direction. The scheme uses 4^{th} order polynomials in the x- and y- directions, and a 2^{nd} order polynomial in the z- direction, in order to save extra computing time due to the variable vertical grid spacing. To deal with the CFL criterion the scheme is run three times inside one dynamic time step and the Courant number is checked for each direction at each internal time step. Both the upstream form and the constant grid flux form of the Bott scheme may be used by changing the values of the coefficients used in the polynomials. The upstream form having weaker mass conservation properties, only results obtained with the constant grid flux form are presented here.

Though the Bott scheme needs a larger amount of calculations, its combination with the semi-Lagrangian model allows longer dynamic time steps, and thus yields a relative low computational cost. Compared to the cost of the pure semi-Lagrangian scheme, the present procedure needs only 8% longer time, and moreover, it is still 59% cheaper than the Eulerian central difference scheme.

5.3.3 Results.

The Bott scheme has been tested as previously on simulations of the ETEX release. One first result is the variation of the *average concentration* shown on figure 10. In the present simulation, diffusion processes have been removed in order to investigate the properties of the advection scheme alone. Contrasting with the previous simulations, the *average concentration* of passive tracers, after the end of the emission phase, remains constant during almost 40 hours, and then it starts to decrease when the passive tracers field reaches the borders of the model area. Nevertheless, the total amount of passive tracers still exceeds the actual quantity (but by only 1.4 time). This is due to the approximation mentioned earlier about equidistant grid spacing, as it will be discussed later. This better behaviour during most of the simulation length confirms the major improvement of the Bott scheme as regards the mass conservation requirement during advection of passive tracers.

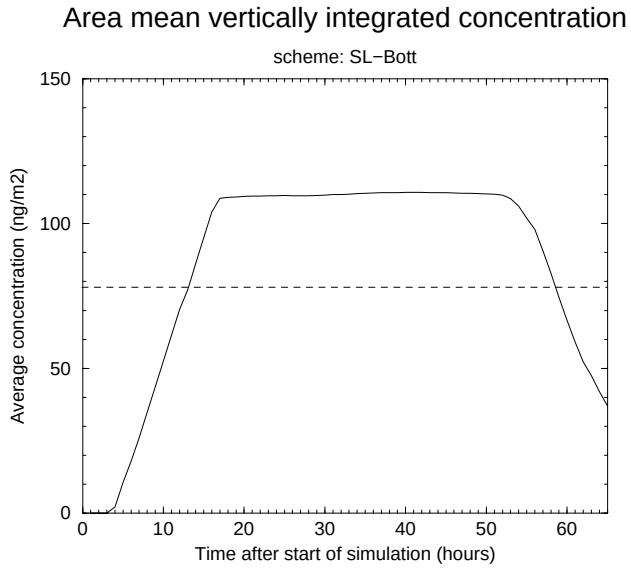

Figure 10 : Evolution of the total amount of passive tracers during a simulation with the Bott advection scheme.

Figure 11 presents the corresponding modelled surface concentration forecast at 24 and 48 hours after start of release obtained in the conditions used in fig.10, that is, without any diffusion and with the Bott scheme applied to the passive tracers. Despite the good performance concerning the mass conservation of this simulation, the modelled surface concentrations do not resemble the observations ; the concentration values are too high and the shape of the cloud is too compact.

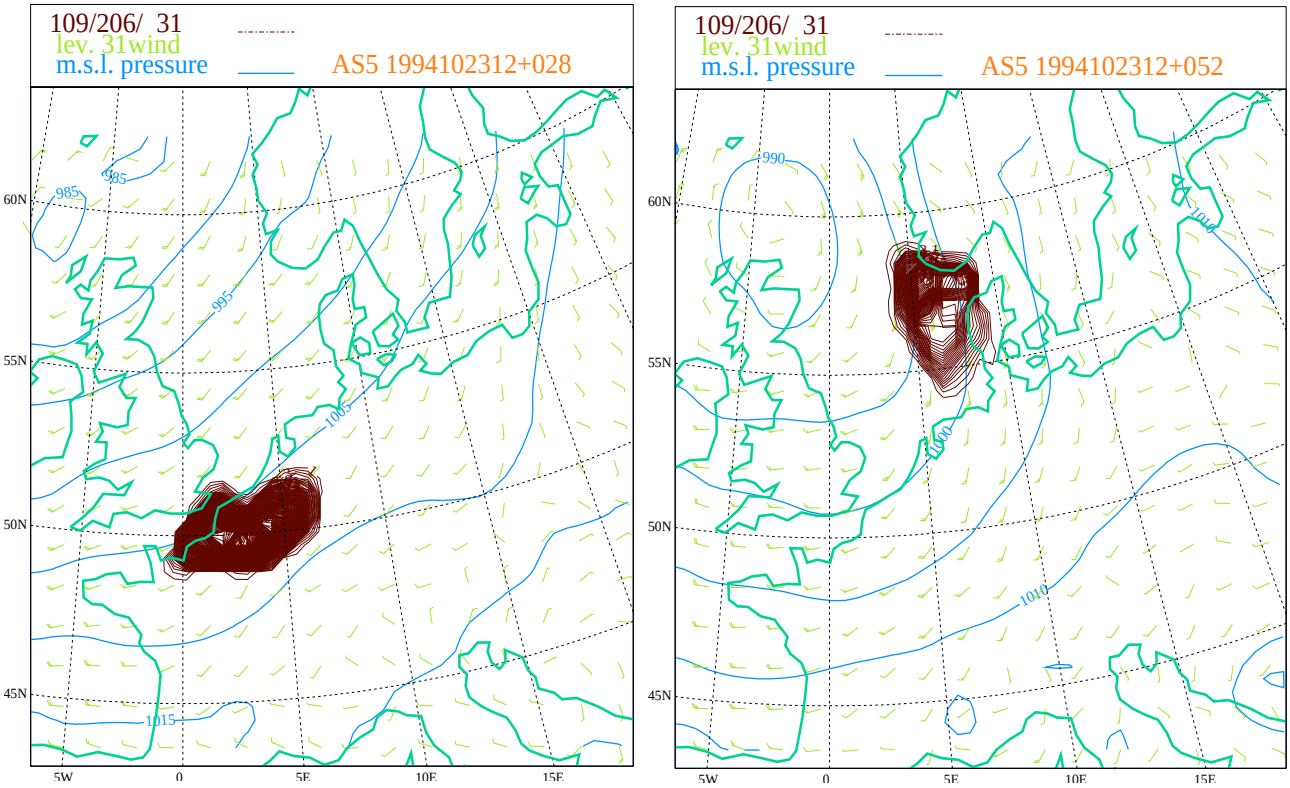

Figure 11 : Surface modelled concentration at 24 hours and 48 hours after start of the release with the Bott scheme alone ; the maximum concentrations on the surface are 121 ng/m^3 and 56 ng/m^3, respectively.

The preceding simulation is repeated by including the CBR scheme for the vertical diffusion and also a 4th order implicit filtering to simulate horizontal diffusion. Figure 12 displays the modelled surface concentration thus obtained. Compared to the observations, the shape and the location of the passive tracers field are better; the concentration values are divided by a factor 22 and are close to the measurements.

Figure 13 compares the progresses of the *average concentration*s obtained during simulations using the Bott scheme either with or without horizontal and vertical diffusion.
Figure 14 presents the corresponding variations of the one-hour average surface concentration at Risø compared to the measurements.

Note that the *average concentration* variation obtained with the Bott scheme together with the CBR scheme is very similar to the one obtained in fig.10 with the Bott scheme alone, and it is also the closest to the ideal *average concentration* level. Moreover, it is the same simulation which yields the best modelled surface concentration according to the measurements at Risø. This indicates that the CBR scheme is also mass conservative, while the horizontal diffusion scheme used here is not.

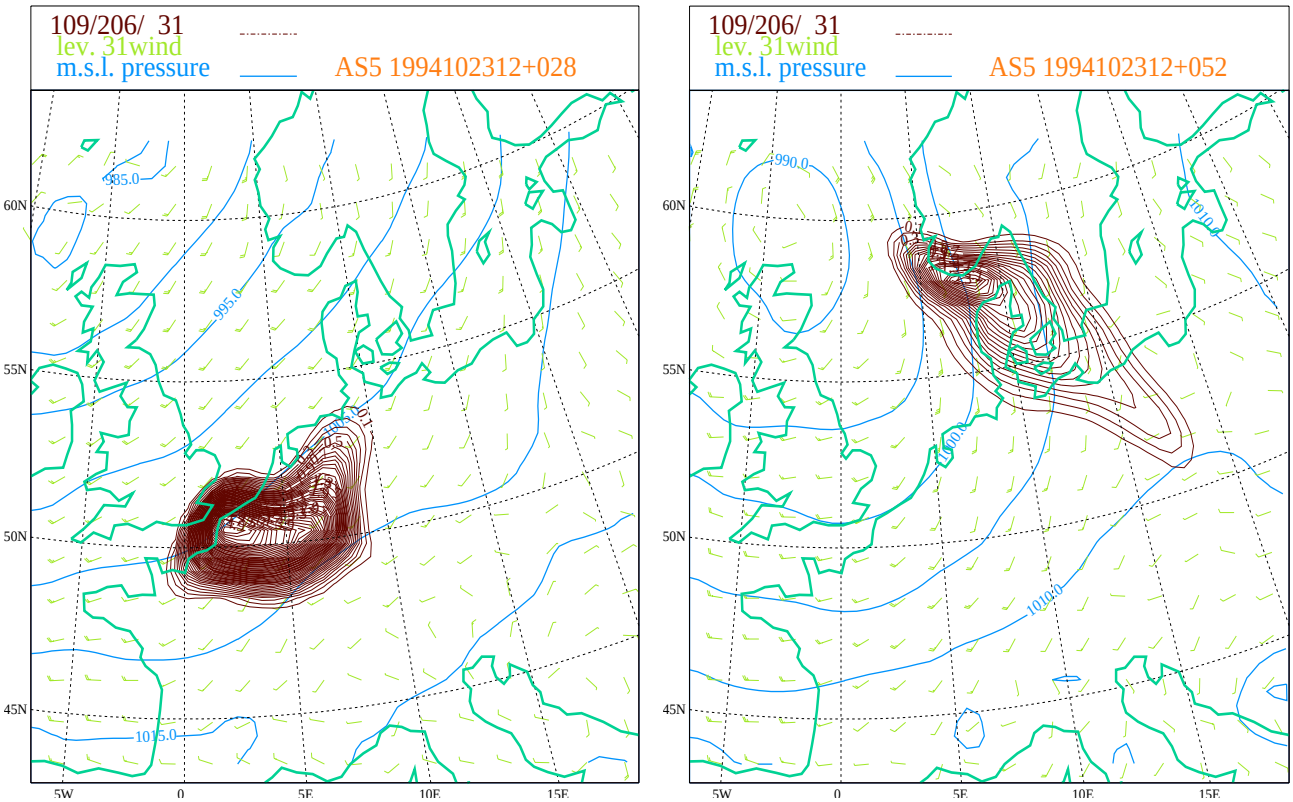

Figure 12 : Same as fig.11 with the Bott scheme used together with vertical and horizontal diffusion ; the maximum concentrations on the surface are 5,1 ng/m^3 and 2,6 ng/m^3, respectively.

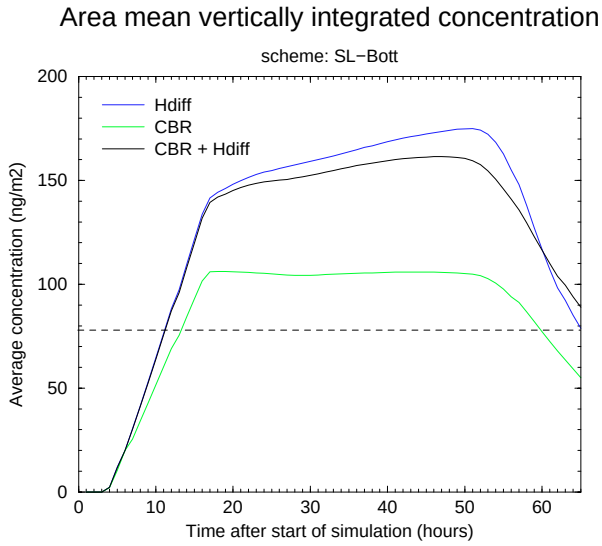

Figure 13 : Comparative progresses of the total amount of passive tracers during simulations with the Bott advection scheme using horizontal and/or vertical diffusion. The horizontal dashed line shows the level corresponding to the total amount of emitted passive tracers.

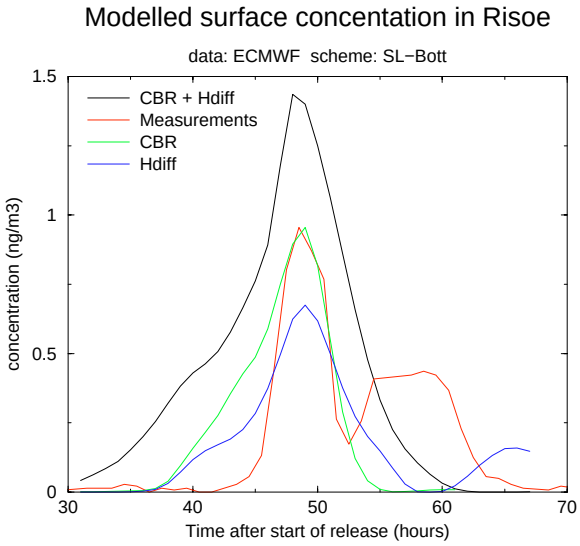

Figure 14 : Comparative variations of one-hour average surface concentration at Risø with the Bott advection scheme using horizontal and/or vertical diffusion. The background concentration has been subtracted from the observations.

6. Discussion and conclusions

Comparison of surface concentration measurements [9] and results from other models [10] with the results obtained in section 4.2.1 shows the poor performances, both qualitatively and quantitatively, of the default transport scheme used in the first version of TRACER. However, modelled surface concentration results may depend on the background meteorological data (quality and/or resolution) used for the simulations. Nevertheless, the same conclusion can be drawn when using an intrinsic criterion like the mass conservation property, which the simplest way to check it, is to look at the progress of the total amount of passive tracers during the simulation. We have seen that the Eulerian central difference scheme does not respect this criterion, yielding a continuous increase of the *average concentration* even after the end of the emission and an important excess of the total mass. The reason for this is that, in the original Eulerian central difference scheme, unrealistic negative values may appear for quantities with sharp gradients ; in order to preserve positive definite quantities, such negative values are set to zero. Tests of the linearity of the model have been performed by simulating the ETEX release with a double emission rate of passive tracers. The results obtained show an increased amount of passive tracers by a factor higher than three. Results obtained by using the semi-Lagrangian model version of HIRLAM are even worse, in particularly as regards the mass conservation requirement, because no negative values are neither allowed in the semi-Lagrangian model for positive definite quantities. It has been showed [6] that this resetting procedure may distort the mass budget of the constituents. Such a behaviour, even if it may not be consequential for simulation of the meteorological fields, is unacceptable for modelling of pollution transport, where mass conservation (as well as the property of monotonicity) is of the highest importance [17].

Among the advection schemes used here only the Bott scheme presents an *average concentration* with a regular increase during the emission phase followed by a constant value during most of the forecast period when the passive tracer field is advected in the model domain ; this may be due to the absence of physical diffusion during the simulation, but it also denotes the non-existence of numerical diffusion in the scheme. It is particularly interesting to note that almost the same behaviour remains when applying the CBR scheme for the vertical diffusion together with the Bott scheme. Nevertheless, adding horizontal diffusion processes has shown an important augmentation (more than 30%) of the total mass budget, followed by a slight increase during transport (cf. Figure 13) ; this would indicate that the horizontal diffusion terms contain some errors regarding mass conservation. Besides, the Bott scheme has demonstrated good continuity abilities in every case. However, the total amount of passive tracers exceeds the actual quantity emitted in the model. This is due to the use of the area preserving polynomial coefficients given in [5], which are obtained by assuming equidistant grid spacing. This approximation turns out to be a little too rough when using HIRLAM, as here, with a lower horizontal resolution than 0.4°. Indeed, preliminary results obtained by using more accurate meteorological data with a higher horizontal resolution show a complete resolving of this problem, and the mass conservation requirement is then absolutely fulfilled.

Furthermore, it is obvious that using vertical diffusion improves the modelled surface concentration field. For example in the case of the Eulerian central difference scheme, the comparison between figures 1 and 3 (right), which only differ by the use of the CBR scheme for the vertical diffusion, obviously shows the improvement of the result in the 2nd case. Indeed, the shape obtained in figure 3 looks like the shape given at the same date by other models like, for example, DERMA [18] and DREAM [19]. The vertical diffusion has also a positive effect on the modelled maximum concentration which converges to a value of a

few ng/m^3 on the surface, independently on the advection scheme used. This is confirmed by the measurements at Risø, where the centre (highest surface concentration) of the ETEX cloud actually arrived 48 hours after the start of the release [9,10].
Moreover, increasing the strength of the horizontal diffusion in the Eulerian simulations has shown to decrease the value of the maximum concentration and also to weakly extend the passive tracers cloud, which thus slightly dilates the curve of the concentration variations at Risø. Though the shape of the passive tracers cloud obtained with the last Eulerian simulations is rather close to the observations, the modelled surface concentration at Risø remains too high and too long in time. The best results are obtained with the Bott scheme giving values very close to the measurements, but for which the passive tracers cloud, according to the observations [9] after 48 hours, does not extend far enough toward the South. However, the comparison with the measurements showing a double-peak structure at Risø presents some important differences. This, again, may be due to the relatively coarse resolution of the data used here, i.e. initial meteorological fields and lateral boundary updates from ECWMF with 0.5° resolution, which may be not enough to detect this structure.

In conclusion, the present tests of the TRACER model have shown that, when including vertical diffusion processes for the passive tracers, it can be used for transport modelling. The vertical diffusion schemes used here are the same as the ones used for cloud water, and hence are assumed to be mass conserving and thus reliable for transport of scalar quantities like chemical constituents and any other pollutants. The schemes used here to simulate horizontal diffusion processes have not really been investigated, except for the influence of the vertical profile of the horizontal diffusivity coefficient. This is thought to be of minor importance since the horizontal diffusion, operating mainly on very short distances, is mostly assumed to be an artificial process. Though they do not seem to be mass conserving, the horizontal diffusion schemes have primarily been employed here to smooth the sharp gradients produced by the local emission source.
Major improvements of TRACER have been obtained by applying the Bott scheme to the advection. It presents the primal advantage of being mass conservative and thus yields good quantitative results, especially when vertical diffusion is added, as shown in the present work. It has also been showed that using horizontal diffusion together with the Bott scheme corrupts its mass conservation properties ; one should thus avoid to add horizontal diffusion to the Bott scheme. One of the principal outcomes of this work is that the Bott scheme used inside the semi-Lagrangian model yields only 1.08 longer computation time than the semi-Lagrangian scheme alone, and it is even 1.6 times as faster as the Eulerian central difference scheme. Better results are thus obtained in a shorter time than with the default setting of TRACER. It is worth hoping that this behaviour will remain when using several passive tracer fields.
However, the version of the Bott scheme used here is the first published by its author in 1989 [4,5] and improvements of the scheme, which correct some amplitude and phase speed errors, as well as errors related to the time-splitting for multidimensional modelling, have been published in 1992 [20], where the non-linear positive-definite flux limitation is replaced by new monotone flux limiters, and in 1993 [21]. As suggested by [17], new modifications of the original Bott scheme [22] should be easily implemented in the current version of TRACER ; on a longer term, it would be wise to use the most recent version of the Bott scheme.

The next step of this work should be to improve the quantitative performances of the model and confront the results with quantitative outcomes of other models as e.g. DERMA. This will necessitate more accurate data by using initial meteorological fields and 6-hour lateral boundaries updates from HIRLAM with a resolution of 0.2° (about 21km × 22km). As already

mentioned, preliminary results have been obtained which confirm the conclusions drawn here and even show an improvement of the mass conservation, but these simulations are much more expensive in computation time.

Other simulations than the ETEX release which have not been presented here were performed. There was the 2nd ETEX release which took place about 3 weeks after ETEX-1. The simulations of ETEX-2 gave results that present the same characteristics as discussed here.
More recently there has been an exercise organised by RTMOD [23] simulating a release from Scotland on June 10th 1999 (experience 4). Though this exercise was not designed for passive tracers (because of deposition parameters included in this simulation), the results obtained with the Eulerian central difference scheme and vertical diffusion gave results pretty close to those obtained with DERMA. The most interesting outcome of this exercise was to experience the ability of using the present work for future real-time experiments by running the model in an operational forecast mode.
This also points out the necessity to include other physical and chemical processes in the model, like for example dry and wet depositions terms added to the advection-diffusion equation. In the same way, one may apply the model on nuclear accidental releases, like for example, the recent release of Cs-137 from Algeciras (Spain) that occurred on May 30th 1998.
The results of all these simulations should be compared to simulations made with other Eulerian models like, e.g. MM5 (MCCM).

Acknowledgements

This work would not have been possible without the help of Jess-Ulrik Jørgensen who is acknowledged for his technical assistance with the recoded version of DMI-HIRLAM. I am extremely grateful to Jens Havskov Sørensen for very stimulating discussions, as well as Alexander Baklanov, Leif Laursen, Bennert Machenhauer and Xiang-Yu Huang for their critical reading of the manuscript. Thanks to Bent Hansen Sass and Niels Woetmann Nielsen for their helpful advice. I would like to thank Annica Ekman from MISU for her code of the Bott's advection scheme and also for her help during the implementing phase.

References

[1] Sørensen J.H., Sensitivity of the DERMA long-range Gaussian dispersion model to meteorological input and diffusion parameters, Atmos. Env. 32, 4195-4206, 1998.
[2] Jensen M.H., Rasmussen A., Svenmark H., Sørensen J.H., Danish Atmospheric Chemistry Forecasting System, DMI, Technical Report 96-3.
[3] Sørensen J.H., Operational dispersion program, Version 1, Documentation manual, DMI, Technical Report 93-5.
[4] Bott A., A positive definite advection scheme obtained by non-linear renormalization of the advective fluxes, Mon. Wea. Rev., 117, 1006-1015, 1989.
[5] Bott A., Reply, Mon. Wea. Rev., 117, 2633-2636, 1989.
[6] Ekman A. and Källen E., Mass conservation tests with the HIRLAM semi-Lagrangian time integration scheme, HIRLAM Technical Report N°39, 1998.
[7] Ekman A., MISU, Sweden, Private communication.
[8] Jørgensen J.U., DMI, Denmark, Personal communication.

[9] Graziani G., Klug W., Mosca S., Real-Time Long-Range Dispersion Model Evaluation of the ETEX first Release, Office for Official Publications of the European Communities, 1998.
[10] Tveten U. and Mikkelsen T., Eds., Report of the Nordic Dispersion-Trajectory Model Comparison with the ETEX-1 Fullscale Experiment, Risø-R-847(EN), 1995.
[11] HIRLAM documentation manual, System 2.5, Ed. E. Källen, 1996.
[12] Holtslag A. M. M. and Moeng C.-M., Eddy diffusivity and countergradient transport in the convective atmospheric boundary layer, J. Atmos. Sci. Bf 48, 1690-1698, 1991.
[13] Cuxart J., Bougeault P., Redelsperger J.-L., A turbulence scheme allowing for mesoscale and large eddy simulations, Q. J. R. Meteorol. Soc. XXX, 1-22, 1999.
[14] McDonald A., The HIRLAM two time level, three dimensional semi-Lagrangian, semi-implicit, limited area, grid point model of the primitive equations, HIRLAM Technical Report N°17, 1994.
[15] Kaas E., The Construction of and Tests with a Multi-level Semi-Lagrangian and Semi-Implicit Limited Area Model, Master Thesis, University of Copenhagen, 1987.
[16] Pietrzak J., A comparison of advection schemes for ocean modelling, DMI, Scientific Report, 95-8.
[17] Baklanov A., DMI, Denmark, Research notes on the advection schemes for passive scalars in the HIRLAM model, 5p., 2000.
[18] Sørensen J.H., Rasmussen A., Ellermann T., Lyck E., Mesoscale influence on long-range transport - Evidence from ETEX modelling and observations, Atmos. Env. 32, 4207-4217, 1998.
[19] Brandt J., Modelling Transport, Dispersion and Deposition of Passive Tracers from Accidental Releases, PhD thesis, NERI, 1998.
[20] Bott A., Monotone flux limitation in the area-preserving flux-form advection algorithm. *Monthly Weather Review*, 120 (11): 2592-2602, 1992.
[21] Bott A., The monotone area-preserving flux-form advection algorithm: reducing the time-splitting error in two-dimensional flow fields. *Monthly Weather Review*, 121 (9): 2637-2641, 1993.
[22] Easter R.C., Two modified versions of Bott's positive-definite numerical advection scheme. *Monthly Weather Review*, 121 (1): 297-304, 1993.
[23] Graziani G., Galmarini S., Mikkelsen T., RTMOD: Real-Time MODel Evaluation, Risø - R-1174(EN), JRC - Ispra Report TN.I.0011, 2000.

DANISH METEOROLOGICAL INSTITUTE

Scientific Reports

Scientific reports from the Danish Meteorological Institute cover a variety of geophysical fields, i.e. meteorology (including climatology), oceanography, subjects on air and sea pollution, geomagnetism, solar-terrestrial physics, and physics of the middle and upper atmosphere.

Reports in the series within the last five years:

No. 95-1
Peter Stauning and T.J. Rosenberg:
High-Latitude, day-time absorption spike events
1. morphology and occurrence statistics
Not published

No. 95-2
Niels Larsen: Modelling of changes in stratospheric ozone and other trace gases due to the emission changes : CEC Environment Program Contract No. EV5V-CT92-0079. Contribution to the final report

No. 95-3
Niels Larsen, Bjørn Knudsen, Paul Eriksen, Ib Steen Mikkelsen, Signe Bech Andersen and Torben Stockflet Jørgensen: Investigations of ozone, aerosols, and clouds in the arctic stratosphere : CEC Environment Program Contract No. EV5V-CT92-0074. Contribution to the final report

No. 95-4
Per Høeg and Stig Syndergaard: Study of the derivation of atmospheric properties using radio-occultation technique

No. 95-5
Xiao-Ding Yu, **Xiang-Yu Huang** and **Leif Laursen** and Erik Rasmussen: Application of the HIRLAM system in China: heavy rain forecast experiments in Yangtze River Region

No. 95-6
Bent Hansen Sass: A numerical forecasting system for the prediction of slippery roads

No. 95-7
Per Høeg: Proceeding of URSI International Conference, Working Group AFG1 Copenhagen, June 1995. Atmospheric research and applications using observations based on the GPS/GLONASS System
Not published

No. 95-8
Julie D. Pietrzak: A comparison of advection schemes for ocean modelling
No. 96-1
Poul Frich (co-ordinator), H. Alexandersson, J. Ashcroft, B. Dahlström, G.R. Demarée, A. Drebs, A.F.V. van Engelen, E.J. Førland, I. Hanssen-Bauer, R. Heino, T. Jónsson, K. Jonasson, L. Keegan, P.Ø. Nordli, **T. Schmith**, **P. Steffensen**, H. Tuomenvirta, O.E. Tveito: North Atlantic Climatological Dataset (NACD Version 1) - Final report

No. 96-2
Georg Kjærgaard Andreasen: Daily response of high-latitude current systems to solar wind variations: application of robust multiple regression. Methods on Godhavn magnetometer data

No. 96-3
Jacob Woge Nielsen, Karsten Bolding Kristensen, Lonny Hansen: Extreme sea level highs: a statistical tide gauge data study

No. 96-4
Jens Hesselbjerg Christensen, Ole Bøssing Christensen, Philippe Lopez, Erik van Meijgaard, Michael Botzet: The HIRLAM4 Regional Atmospheric Climate Model

No. 96-5
Xiang-Yu Huang: Horizontal diffusion and filtering in a mesoscale numerical weather prediction model

No. 96-6
Henrik Svensmark and Eigil Friis-Christensen: Variation of cosmic ray flux and global cloud coverage - a missing link in solar-climate relationships

No. 96-7
Jens Havskov Sørensen and Christian Ødum Jensen: A computer system for the management of epidemiological data and prediction of risk and economic consequences during outbreaks of foot-

and-mouth disease. CEC AIR Programme. Contract No. AIR3 - CT92-0652

No. 96-8
Jens Havskov Sørensen: Quasi-automatic of input for LINCOM and RIMPUFF, and output conversion. CEC AIR Programme. Contract No. AIR3 - CT92-0652

No. 96-9
Rashpal S. Gill and Hans H. Valeur:
Evaluation of the radarsat imagery for the operational mapping of sea ice around Greenland

No. 96-10
Jens Hesselbjerg Christensen, Bennert Machenhauer, Richard G. Jones, Christoph Schär, Paolo Michele Ruti, Manuel Castro and Guido Visconti:
Validation of present-day regional climate simulations over Europe: LAM simulations with observed boundary conditions

No. 96-11
Niels Larsen, Bjørn Knudsen, Paul Eriksen, Ib Steen Mikkelsen, Signe Bech Andersen and Torben Stockflet Jørgensen: European Stratospheric Monitoring Stations in the Artic: An European contribution to the Network for Detection of Stratospheric Change (NDSC): CEC Environment Programme Contract EV5V-CT93-0333: DMI contribution to the final report

No. 96-12
Niels Larsen: Effects of heterogeneous chemistry on the composition of the stratosphere: CEC Environment Programme Contract EV5V-CT93-0349: DMI contribution to the final report

No. 97-1
E. Friis Christensen og C. Skøtt: Contributions from the International Science Team. The Ørsted Mission - a pre-launch compendium

No. 97-2
Alix Rasmussen, Sissi Kiilsholm, Jens Havskov Sørensen, Ib Steen Mikkelsen: Analysis of tropospheric ozone measurements in Greenland: Contract No. EV5V-CT93-0318 (DG 12 DTEE): DMI's contribution to CEC Final Report Arctic Trophospheric Ozone Chemistry ARCTOC

No. 97-3
Peter Thejll: A search for effects of external events on terrestrial atmospheric pressure: cosmic rays

No. 97-4
Peter Thejll: A search for effects of external events on terrestrial atmospheric pressure: sector boundary crossings

No. 97-5
Knud Lassen: Twentieth century retreat of sea-ice in the Greenland Sea

No. 98-1
Niels Woetman Nielsen, Bjarne Amstrup, Jess U. Jørgensen:
HIRLAM 2.5 parallel tests at DMI: sensitivity to type of schemes for turbulence, moist processes and advection

No. 98-2
Per Høeg, Georg Bergeton Larsen, Hans-Henrik Benzon, Stig Syndergaard, Mette Dahl Mortensen: The GPSOS project
Algorithm functional design and analysis of ionosphere, stratosphere and troposphere observations

No. 98-3
Mette Dahl Mortensen, Per Høeg:
Satellite atmosphere profiling retrieval in a nonlinear troposphere
Previously entitled: Limitations induced by Multipath

No. 98-4
Mette Dahl Mortensen, Per Høeg:
Resolution properties in atmospheric profiling with GPS

No. 98-5
R.S. Gill and M. K. Rosengren
Evaluation of the Radarsat imagery for the operational mapping of sea ice around Greenland in 1997

No. 98-6
R.S. Gill, H.H. Valeur, P. Nielsen and K.Q. Hansen: Using ERS SAR images in the operational mapping of sea ice in the Greenland waters: final report for ESA-ESRIN's: pilot projekt no. PP2.PP2.DK2 and 2nd announcement of opportunity for the exploitation of ERS data projekt No. AO2..DK 102

No. 98-7
Per Høeg et al.: GPS Atmosphere profiling methods and error assessments

No. 98-8
H. Svensmark, N. Woetmann Nielsen and A.M. Sempreviva: Large scale soft and hard turbulent states of the atmosphere

No. 98-9
Philippe Lopez, Eigil Kaas and Annette Guldberg: The full particle-in-cell advection scheme in spherical geometry

No. 98-10
H. Svensmark: Influence of cosmic rays on earth's climate

No. 98-11
Peter Thejll and Henrik Svensmark: Notes on the method of normalized multivariate regression

No. 98-12
K. Lassen: Extent of sea ice in the Greenland Sea 1877-1997: an extension of DMI Scientific Report 97-5

No. 98-13
Niels Larsen, Alberto Adriani and Guido DiDonfrancesco: Microphysical analysis of polar stratospheric clouds observed by lidar at McMurdo, Antarctica

No.98-14
Mette Dahl Mortensen: The back-propagation method for inversion of radio occultation data

No. 98-15
Xiang-Yu Huang: Variational analysis using spatial filters

No. 99-1
Henrik Feddersen: Project on prediction of climate variations on seasonel to interannual timescales (PROVOST) EU contract ENVA4-CT95-0109: DMI contribution to the final report:Statistical analysis and post-processing of uncoupled PROVOST simulations

No. 99-2
Wilhelm May: A time-slice experiment with the ECHAM4 A-GCM at high resolution: the experimental design and the assessment of climate change as compared to a greenhouse gas experiment with ECHAM4/OPYC at low resolution

No. 99-3
Niels Larsen et al.: European stratospheric monitoring stations in the Artic II: CEC Environment and Climate Programme Contract ENV4-CT95-0136. DMI Contributions to the project

No. 99-4
Alexander Baklanov: Parameterisation of the deposition processes and radioactive decay: a review and some preliminary results with the DERMA model

No. 99-5
Mette Dahl Mortensen: Non-linear high resolution inversion of radio occultation data

No. 99-6
Stig Syndergaard: Retrieval analysis and methodologies in atmospheric limb sounding using the GNSS radio occultation technique

No. 99-7
Jun She, Jacob Woge Nielsen: Operational wave forecasts over the Baltic and North Sea

No. 99-8
Henrik Feddersen: Monthly temperature forecasts for Denmark - statistical or dynamical?

No. 99-9
P. Thejll, K. Lassen: Solar forcing of the Northern hemisphere air temperature: new data

No. 99-10
Torben Stockflet Jørgensen, Aksel Walløe Hansen: Comment on "Variation of cosmic ray flux and global coverage - a missing link in solar-climate relationships" by Henrik Svensmark and Eigil Friis-Christensen

No. 99-11
Mette Dahl Meincke: Inversion methods for atmospheric profiling with GPS occultations

No. 99-12
Benzon, Hans-Henrik; Olsen, Laust: Simulations of current density measurements with a Faraday Current Meter and a magnetometer

No. 00-01
Høeg, P.; Leppelmeier, G: ACE: Atmosphere Climate Experiment: proposers of the mission

No. 00-02
Høeg, P.: FACE-IT: Field-Aligned Current Experiment in the Ionosphere and Thermosphere

No. 00-03
Allan Gross: Surface ozone and tropospheric chemistry with applications to regional air quality modeling. PhD thesis

No. 00-04
Henrik Vedel: Conversion of WGS84 geometric heights to NWP model HIRLAM geopotential heights

No. 00-05
Jérôme Chenevez: Advection experiments with DMI-Hirlam-Tracer

No. 00-06
Niels Larsen: Polar stratospheric clouds micro-physical and optical models

No. 00-09
Niels Larsen, Bjørn M. Knudsen, Michael Gauss og Giovanni Pitari: Effects from high-speed civil traffic aircraft emissions on polar stratospheric clouds.